DETERMINATION OF SPRAY DRIFT CHARACTERISTICS OF A RONNIE BAUGH TRACTOR-TRAILED BOOM SPRAYER USING COMPUTATIONAL FLUID DYNAMICS

Abel Francis B. Laguardia[1], Arthur L. Fajardo[1], Omar F. Zubia[1], Ronnie C. Valencia[2], Ralph Kristoffer B. Gallegos[1*]

[1*]Corresponding author. Institute of Agricultural and Biosystems Engineering, University of the Philippines Los Baños /College, Laguna, Philippines. E-mail: rbgallegos@up.edu.ph | ORCID ID: https://orcid.org/0000-0001-8217-6314

ABSTRACT

Spray drift leads to wastage of spraying material and poses a threat to non-targeted crops and the environment. Therefore, the spray drift characteristics of a Ronnie Baugh (RB) tractor-trailed boom sprayer were determined through computational fluid dynamics to assist in designing the tractor for boom spraying with minimized spray drift. The wake region of the RB tractor was characterized by investigating its velocity profile, turbulent kinetic energy, and drag coefficient at different forward speeds. Additionally, spray droplet sizes and drift distances from the boom sprayer were measured at forward speeds of 4, 6, and 8 km/h, along with different wind directions. The RB tractor exhibits an estimated drag coefficient of 0.7. The results further demonstrate that, at varying forward speeds, the wake experiences low turbulent kinetic energy and minimal velocity profile variations. No spray drift was observed at tractor speeds below 4 km/h, whereas a drift of 0.19 m and 0.33 m is predicted at 6 km/h and 8 km/h, respectively. The tractor's wake is significantly influenced by changes in wind direction, resulting in varying drift distances from each nozzle due to exposure to both free and obstructed airflow. To minimize drift at higher travel speeds, it is recommended that the tractor be operated in line with the prevailing wind direction.

INTRODUCTION

Various impacts of pesticide spray drift have been studied over the past ten years. In South Asian countries, pesticides are considered a major contaminant in most of the river systems as their levels exceed the recommended standard limits in water systems, endangering the water's ecosystem (Sarker et al., 2021). Likewise, in the Philippines, there has been a noteworthy rise in both the quantity and frequency of pesticide usage, which raises concern about their impact on human well-being and the environment (Baurdoux et al., 2004). The assessment of Lu (2017) of pesticide-related pollution and occupational health among vegetable farmers in Benguet, revealed that 49% of the farmers complained of illness due to pesticide exposure, leading to prevalent health symptoms such as muscle pain, muscle weakness, and easy fatigability.

Spray drift refers to a portion of the applied pesticide that fails to deposit on the target crop and is lost to non-target ecosystems (Schönenberger et al., 2022). Studies have shown that this is mostly affected by wind speed and nozzle design (Jomantas et al., 2023). Moreover, Chethan et al. (2019) wrote that spray pattern shape and accuracy of nozzle spraying could become faulty over time as influenced by pesticide formulation, nozzle type, orifice material, and operating pressure. Several studies have already addressed spray drift, utilizing mathematical models, field tests, and computer simulations such as computational fluid dynamics (CFD) simulations. These simulations 'solve complex airflow and turbulence patterns by solving the Navier-Stokes equations' (Hong et al., 2021, p.2). The insights and advancements gleaned from prior research have revealed the interconnected influences of spray droplet size, wind velocity, and discharge height in

boom spraying. Tsay et al. (2004) identified optimal operational parameters and investigated the effects of wind velocity and sprayer travel speed on spray drift. Additionally, the studies conducted by Baetens et al. (2007) and Zhong et al. (2020) demonstrated the accuracy of Ansys boom spraying simulations in comparison to experimental tests. Moreover, Al Heidary et al. (2020) utilized air induction nozzles in boom spraying, showing a significant mitigation effect on spray drift.

The Ronnie Baugh tractor represents a relatively new design with only limited existing studies concerning its characteristics and operational aspects and it will be subjected to boom spraying simulations in this study using CFD. The primary objective of this research is to analyze the spray drift characteristics of a trailer-mounted boom sprayer attached to the RB tractor. Specifically, the study aims to ascertain the aerodynamic properties of the RB tractor, evaluate spray drift characteristics across varying forward speeds of the tractor, and examine spray drift attributes under different wind directions.

Among the unexplored facets are the tractor's aerodynamics and its potential impact on boom spraying operations. A significant research gap exists regarding the understanding of spray drift as influenced by tractor aerodynamics. Furthermore, the RB tractor is presently undergoing modifications by the Center for Agri-Fisheries and Biosystems Mechanization (BIOMECH) to better suit the agricultural conditions of the Philippines. This study aims to address these gaps by providing valuable insights into the design enhancement and operation of the RB tractor

for more efficient boom spraying. It will achieve this by identifying optimal wind conditions for spraying operations and determining suitable driving speeds for the tractor through the application of CFD simulations.

MATERIAL AND METHODS

ANSYS Fluent Code Validation

Indirect validation was performed by replicating the spray simulation conducted by Reichard et al. (1992) for particle drift using Ansys Fluent and was validated against experimental data. The choice of the same simulation software for replication aimed to assess the software's accuracy in producing precise results.

Determination of Aerodynamic Characteristics of the RB Tractor at Different Forward Speeds

The simplified model of the RB tractor shown in FIGURE 1 was imported to SpaceClaim and further geometry simplifications were applied. Body sizing methods were used to refine the mesh around the tractor and its wake region. Moreover, the smallest mesh size is 30 mm, and any tractor parts or features smaller than this mesh size were removed. In the simulation set-up, steady-state analysis was used which computed the mean values of quantities measured. The k-omega SST turbulence model was also employed to accurately capture near and far wall turbulence by using both the k-ω model for the inner region of the boundary layer and the k-ε model in the outer boundary layer as per the Ansys Fluent 12.0 Theory Guide.
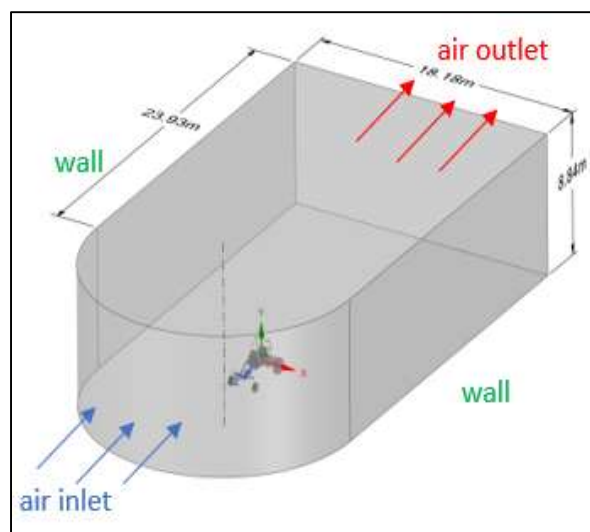

FIGURE 1. Flow domain geometry for tractor aerodynamics characterization.

The air was assumed to be still relative to the traveling tractor at forward speeds of 0.3m/s, 0.7m/s, 1.4 m/s, 1.8 m/s, 2.2 m/s, 2.5 m/s and 2.9 m/s. A coupled scheme of pressure-velocity coupling was used since it obtained an efficient single-phase implementation for steady-state flows. Lastly, CFD-Post was used to investigate velocity and turbulent kinetic energy profiles at the XZ and YZ planes to visualize the wake of the RB tractor from different perspectives. Moreover, the drag coefficient of the RB tractor was also computed by getting the drag force at different forward speeds of the tractor through the CFD-Post table viewer.

Determination of Spray Drift Characteristics at Different Wind Directions and Tractor Forward Speeds

Geometry Setup

Spray drift characteristics were identified first at different forward speeds of the tractor. The computational domain was cut into half along the YZ symmetry plane, as shown in Fig. 2 since the velocity distribution at the left and right sides of the tractor were symmetrical near the ground in which the spray droplets were investigated. The generated mesh was converted to polyhedral in the Ansys Fluent Solver to lower the original cell count and improve the orthogonal quality and skewness of the mesh.
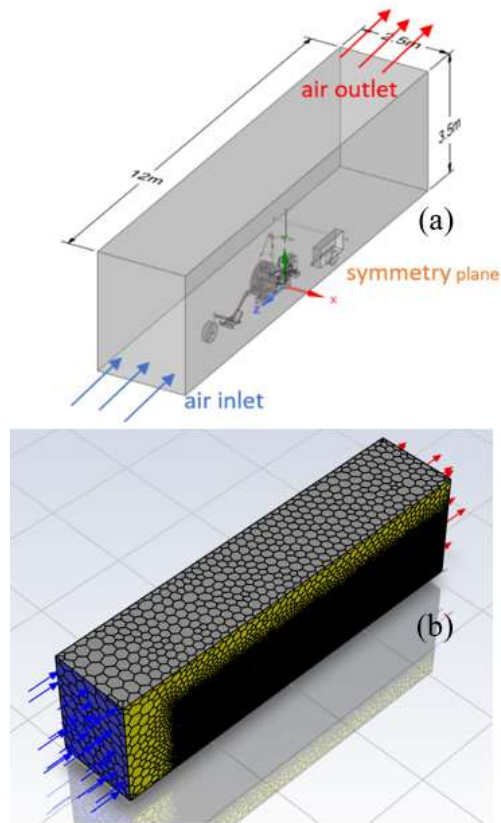
FIGURE 2. Flow domain (a) geometry and (b) mesh for spray drift characterization.

Spray drift was investigated at wind angles of 0°, 45°, 90°, 135°, and 180° clockwise from the positive z-axis as shown in FIGURE 3. The tractor, with a forward speed of 8 km/h, was exposed to a wind speed of 1.5 m/s at different wind angles of attack. The flow domain was reoriented depending on the resultant direction of the wind coming from different angles with respect to the moving tractor at 8 km/h.
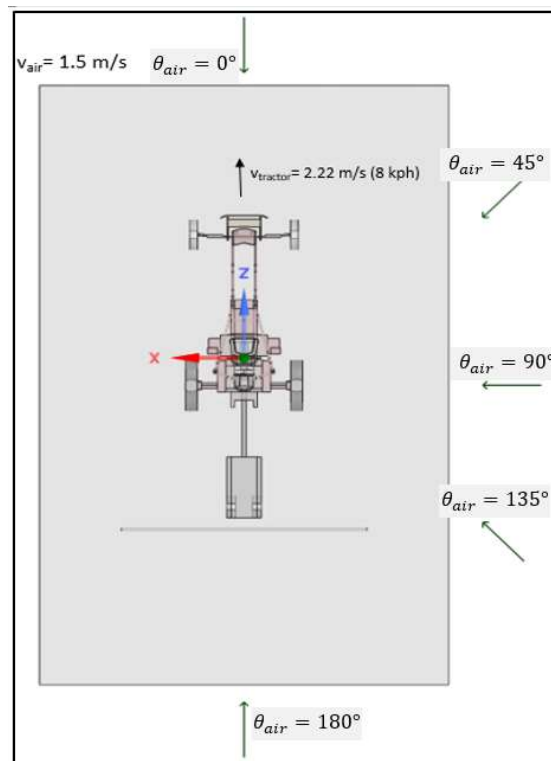

FIGURE 3. Flow domain subjected to different wind direction.

Simulation Setup

The multiphase flow model was also used to incorporate the inhomogeneous flow of the continuous phase, which is the air in the Eulerian frame of reference, and the spray droplets, which consist of the discrete phase in the Lagrangian frame of reference. Solid cone injection type was used and since pesticide solutions are mostly composed of water, liquid properties of water were used to characterize the spray droplets. Similar to the droplet emission model of Djouhri et al. (2023), the nozzles were modelled as point sources along the boom, defined by its x, y, and z locations in the domain. Like in the simulation of Zhong et al. (2020), injection properties were derived from Lechler nozzles due to the comprehensive information available online. The simulation used six Lechler full cone nozzles with an orifice diameter of 0.095 inches at 15 psi with a flow rate of 0.0504 kg/s and injection velocity of 11.04 m/s. The spray droplet size distribution is 200-400 microns. and the spacing of the nozzles is 30 inches which is patterned to the row spacing of corn. Furthermore, the boom height is 0.5 m from the ground. The Discrete Phase Model (DPM) boundary condition of the ground wall is "trap," while the side and top wall have a DPM boundary condition of "reflect." At the outlet, the DPM boundary condition is "escape."

The RB Tractor has a traveling speed of 5.08 km/h on dirt roads with a trailer load of 410 kg as tested by the Agricultural Machinery Testing and Evaluation Center (AMTEC, 2021). On the other hand, the trailed boom sprayer reference for this study has a full weight of 430 kg

at 250-liter capacity. Hence, this study investigated spray drift when the tractor is traveling at 4, 6, and 8 km/h, considering that the weight of the sprayer tank decreases as its content is applied on the field. Phase-coupled SIMPLE algorithm was used in pressure-velocity coupling of the phasic momentum, shared pressure, and phasic volume fraction equations because it can solve a wide range of multiphase flow. Moreover, hybrid initialization was conducted and around 750 iterations were calculated.

CFD Post-processing

Graphs of particle tracks colored by droplet diameter, velocity and drift distance were analyzed for the results and discussion. Furthermore, the x and z components of the farthest drifted droplets were determined using the particle tracks colored by their x and z positions. The velocity profile of the air at different wind directions was visualized using a contour plot and this was analyzed in relation to the drift distances of each nozzle along the boom.

Measurement of Spray Drift Distance

The z-component and x-component of the position of the farthest droplet from the nozzle orifice were measured using the color map of droplet tracks colored by the z and x positions. **Erro! Fonte de referência não encontrada.** shows the drift distance measurement with respect to the covered area of the full cone nozzle at a stationary position. The maximum drift distance (Δd) was computed by subtracting the resultant position (d_R) of the x and z component of the droplet to the radius (d) of the spray coverage area with no drift as shown in [eq. (1)].
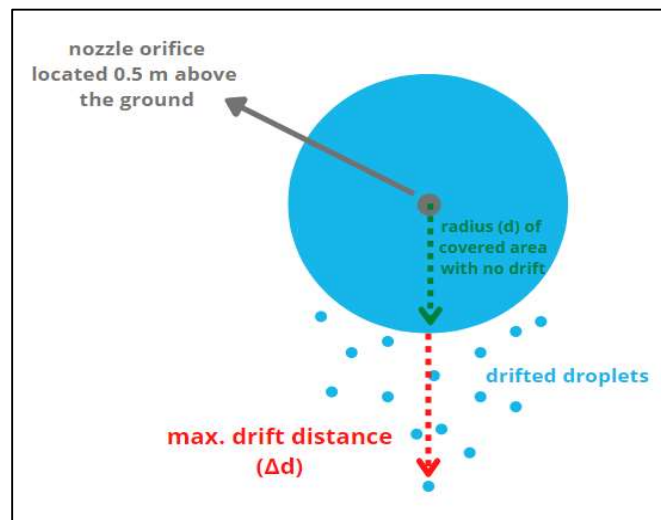

FIGURE 4. Maximum drift distance measurement.

$$\Delta d = d_R - d \tag{1}$$

in which:

Δd - spray drift distance (m);

d_R - displacement of the farthest droplet from the nozzle (m),

d - radius of the spray coverage area with no drift (m).

RESULTS AND DISCUSSION

ANSYS Fluent Code Validation

In TABLE 1, the replicated simulation results show less than 5% difference to the reference data of Reichard et al. (1992) for all settings of wind velocity when the droplet diameter is 100 μm.

TABLE 1. Indirect validation of simulation results.

Droplet diameter (μm)	Wind velocity (m/s)	Reference Mean drift distance (m)	Replicated Mean drift distance (m)	Difference (%)
100	0.5	0.64	0.62	3.23
100	1	1.3	1.24	4.84
100	2	2.6	2.49	4.42
100	4	5.1	4.999	2.02

Determination of Aerodynamic Characteristics of RB Tractor

FIGURE 5 shows the isometric view of the flow domain and YZ planes were positioned at the boom nozzle locations to investigate the turbulent kinetic energy and velocity profile near each nozzle.
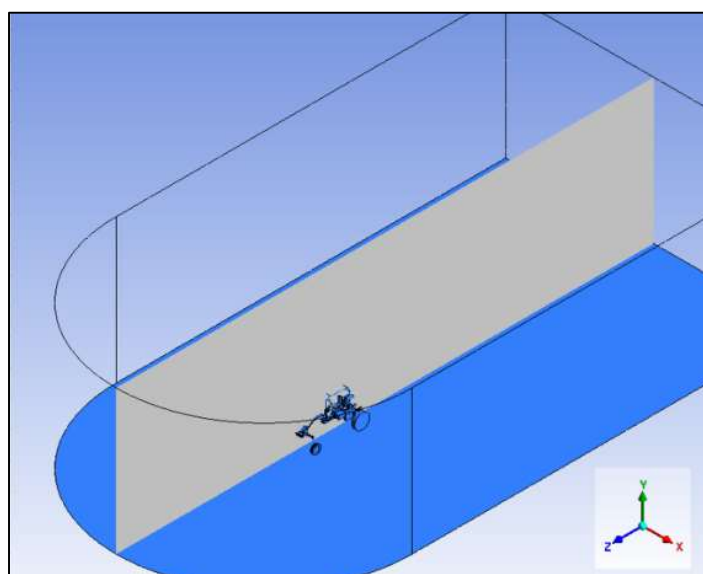

FIGURE 5. Isometric view of the flow domain with YZ symmetry plane.

In FIGURE 6, the wind velocity profile at 0.38 m away from the YZ symmetry plane of the tractor has the most observable changes when the tractor forward speed is increased. The velocity contour plot shows that the velocity gradually decreases in magnitude in the wake of the tractor and as it goes closer to the ground. The ground has a computed roughness height of 0.6 m and a roughness length of 0.03 m for an open agricultural area with no hedge rows and few obstacles (Wieringa, 1992). At a forward speed of 2.9 m/s, the velocity at the wake at the level of the rare wheels drops to around 2 m/s. At 1.14 m and 1.9 m away from the symmetry plane of the tractor, the effect of the tractor obstruction on the wind velocity profile is negligible.

Furthermore, the wake region extends up to around five times the length of the tractor as seen in Figure 7. The velocity decreased by 0.07 m/s, 0.44 m/s, and 0.7 m/s at the wake at a forward speed of 1 km/h, 6.5 km/h, and 10.4 km/h respectively However, the velocity drop at the wake is very small, especially at the recommended boom spraying speed of 4-8 km/h. Moreover, the width of the wake is approximately 2 meters which is the same as the projected width of the tractor.
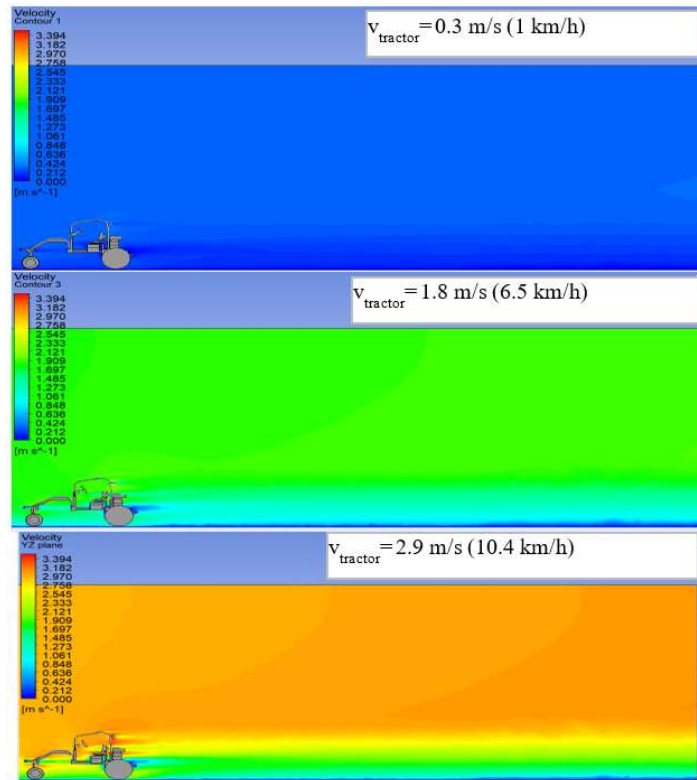
FIGURE 6. Velocity profile at 0.38 m away from YZ plane.

FIGURE 7. Velocity vector near the inlet and outlet of the flow domain at 10.4 km/h forward speed.

In FIGURE 8, the changes in the turbulent kinetic energy (TKE) profile at the wake of the RB tractor are gradual and have minimal variation. The TKE of the air at the wake of the tractor increases when the forward speed is increased from a minimum speed of 1 km/h up to the tractor's top speed of 10.4 km/h. At 0.38 meters away from the YZ symmetry plane, tractor obstruction has a slight influence on the increase of TKE at the wake. The TKE behind the tractor is around 0.001 m^2/s^2, 0.05 m^2/s^2, and 0.20 m^2/s^2 at forward speeds of 1 km/h, 6.5 km/h and 10.4 km/h respectively. The TKE developed at the wake is low due to the slow driving speed of the tractor recommended for boom spraying operation. High turbulent kinetic energy is avoided because it interferes with the flow of the droplet particles which can cause change in the droplet trajectories and the drift distances. Small droplets measuring 100 microns or less are highly prone to drift that is dependent on the irregularities of turbulent air than gravity alone (Kruger et al., 2019).
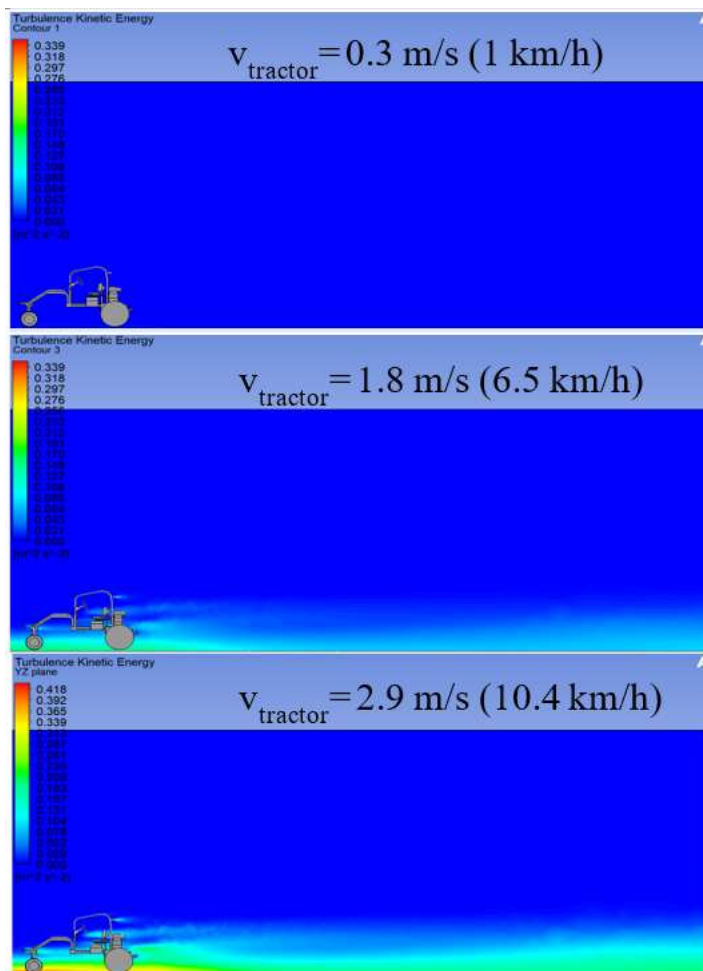
FIGURE 8. TKE profile at 0.38 m away from YZ symmetry plane.

The TKE of the RB tractor at its top speed is close to the computed TKE by Cai et al. (2020) for a truck running at 18 km/h with a TKE value of 0.26 m2/s2. The TKE of the RB tractor running at its top speed of 10.4 km/h is only below 0.25 m^2/s^2 at the wake region where the boom sprayer is positioned which is why the droplets travel at trajectories along the direction of the wind and the droplet flow appears laminar at all setups with different forward tractor forward speeds. The kinetic energy generated is not enough to cause significant turbulence in the movement of the droplets. FIGURE 9 shows that the change in TKE is most pronounced at the tractor's top speed of 10.4 km/h and TKE diminishes as it goes farther behind the wake region. Lower turbulent kinetic energy is developed behind the tractor wheels, and this extends towards the outlet boundary of the domain.
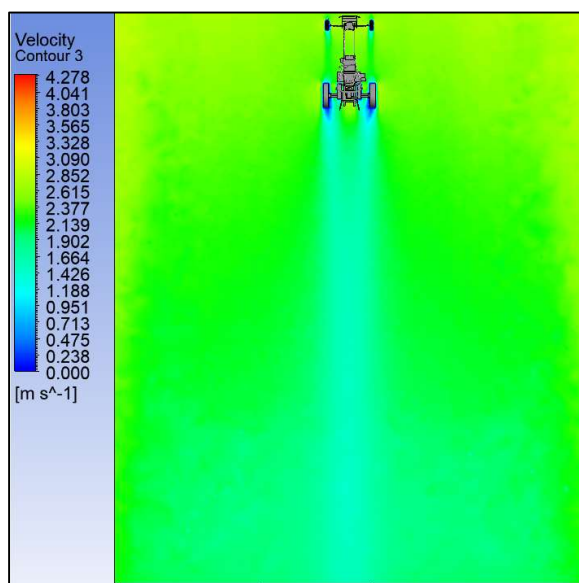

FIGURE 9. XZ plane wind velocity profile at 10.4 km/h forward speed.

Moving on, TABLE 2 presents the simulation results at different forward speeds and their corresponding drag and lift forces. The drag coefficient is defined by [eq. (2)]. To solve for the drag coefficient, a constant ratio of the drag force and the square of velocity was computed first by quadratic regression in the form of [eq. (3)] as the fit method.

$$c_d = \frac{2F_d}{\rho v^2 A} \tag{2}$$

in which:

C_d - drag coefficient;

F_d - drag force parallel to the direction of the wind (N);

ρ - air density at STP (1.225 kg/m³);

v - velocity of the tractor (m/s);

A - projected area of the tractor normal to the wind direction (m²).

$$F_d = m * v^2 \tag{3}$$

in which:

m - constant equal to 0.652507.

TABLE 2. Drag and lift forces at different forward speeds.

Velocity (m/s)	Drag force (N)	Lift force (N)
0.3	0.0587	0.0099
0.7	0.3271	0.0586
1.1	0.7998	0.1484
1.4	1.2900	0.2433
1.8	2.1180	0.4122
2.2	3.1630	0.5973
2.5	4.0800	0.8054
2.9	5.4780	1.0480

As observed in FIGURE 10, the drag produced increases at a parabolic rate as the forward speed of the tractor increases.
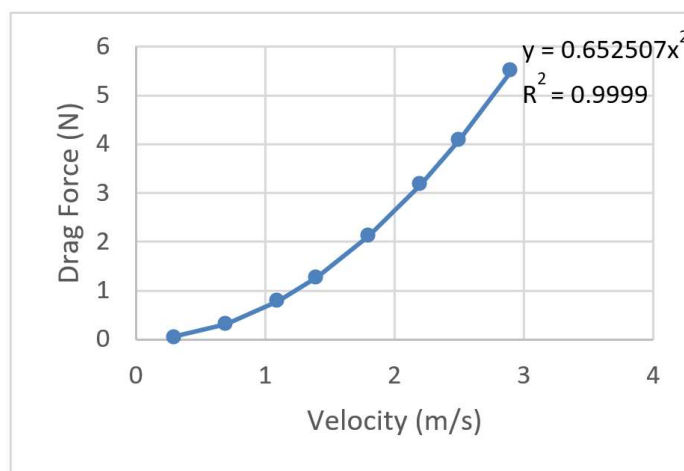

FIGURE 10. Curve fit of drag versus velocity.

Moreover, the frontal projected area of the RB tractor was measured in SpaceClaim with a value of 1.49 m². With all the needed values obtained, the drag coefficient of the RB tractor was solved in [eq. (4)].

$$c_d = \frac{2*m}{\rho A} = \frac{2*0.652507}{1.225\frac{kg}{m^3}*1.4868m^2} = \mathbf{0.72} \tag{4}$$

Sarkar et al. (2019) noted that a higher drag coefficient increases fuel consumption and power loss while reducing the top speed of a vehicle. Eckert et al. (2014) presented different types of vehicles showing that streamlined design vehicles have lower c_d while open convertible cars and motorcycles have higher c_d ranging from 0.5-0.7. The computed c_d of the RB tractor is near this range because of its low projected surface area, just like in bicycles, motorcycles, and cabriolets, which have high c_d values.

Spray Drift Characteristics at Different Forward Speeds

At a boom height of 0.5 meters, spray pressure of 15 psi, and spray angle of 60°, the spray coverage of the full cone nozzle on the ground is 0.21 m² with a radius (d) of 0.26 m. This was the basis for determining the drift distances (Δd) from the nozzle outlets (see Fig. 4). In the simulations, the drift distance of droplets increased as the tractor sped up. At a forward speed of 1.11 m/s (4 km/h) and below, there is no observable drift of droplets (FIGURE 11) and the approximate circular area covered by spraying was preserved.
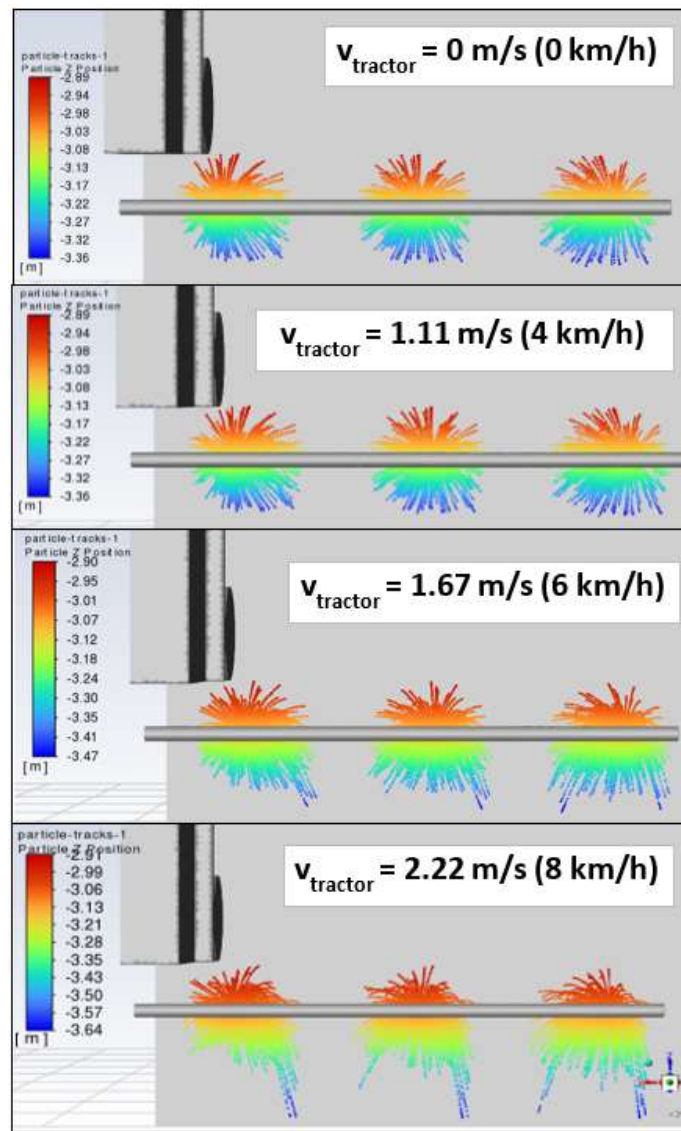
FIGURE 11. Droplet tracks colored by droplet Z position.

This is consistent with the result of Xue et al. (2021), wherein the droplets did not deposit farther away than 2 meters for droplets up to 250 μm at wind speed of 1 m/s and nozzle height can still be adjusted above 5 meters from the ground with little to no drifted spray particles. The airflow generated at the wake was not strong enough to disrupt the trajectories of the spray droplets created by the nozzle pressure. In addition, Musiu et al. (2019) indicated that spray deposition decreases with a decrease in the volumetric flow rate but increases distribution uniformity. As the spraying speed was increased to 6 km/h and 8 km/h, spray drift developed because of the intensified airflow. According to Al Heidary et al. (2014) trajectories of the droplets are modified due to the drag force induced by the air velocity and stronger air velocity increases the drag force

on the spray droplets. The spray coverage area becomes irregular when the forward speed is 1.67 m/s and 2.22 m/s as some of the spray particles change trajectory and drift downstream. The droplets located at the periphery of the covered area were most prone to drift, and this is most observable at a forward speed of 2.22 m/s. At 1.11 m/s, 1.67 m/s, and 2.2 m/s, the spray droplets were deposited furthest at 0.26 m, 0.45 m, and 0.59 m from the nozzle orifice respectively. Subtracting this to d, it was found that the maximum spray drift at forward speeds of 6 km/h and 8 km/h was 0.19 m and 0.33 m, respectively. In Figure 12, the particle droplets colored by particle size diameter show that finer droplets with a diameter of 200 μm drifted farthest from the nozzle outlet.
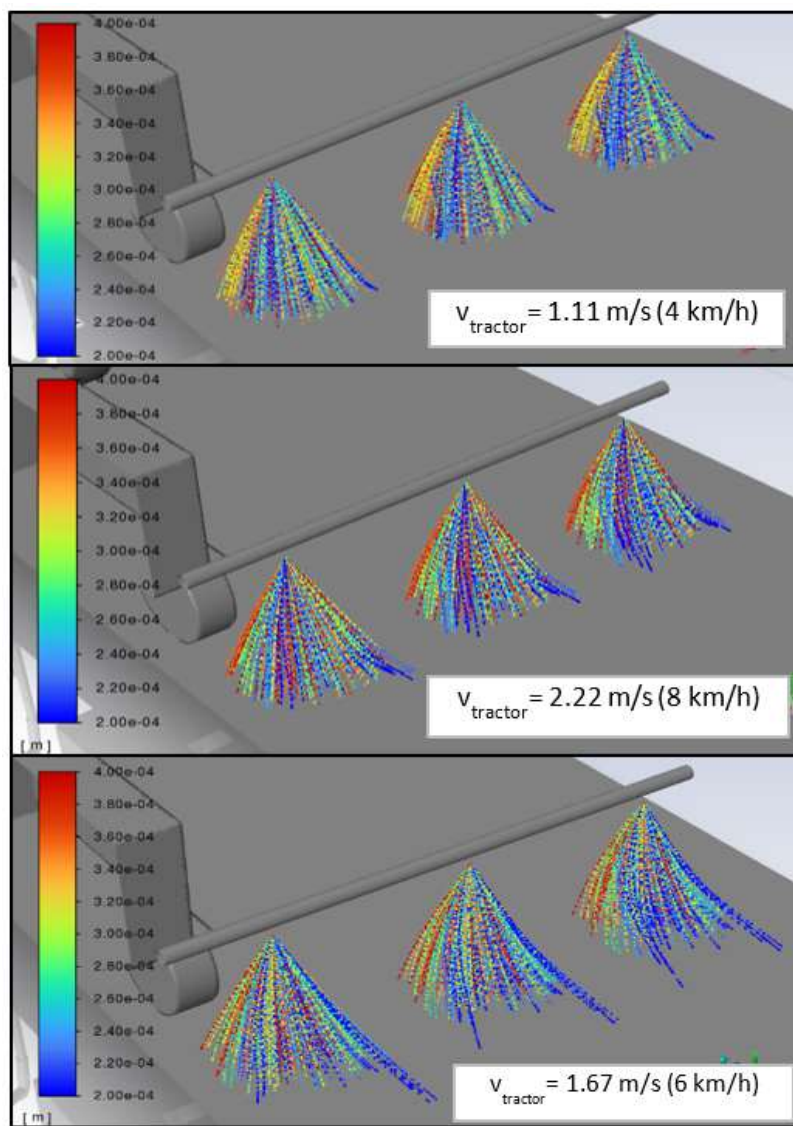
FIGURE 12. Droplet tracks colored by droplet diameter.

On the other hand, coarsest droplets with a diameter of 400 μm were deposited first and were most resistant to being drifted. At different forwards speeds, most spray particles greater than 200 μm were concentrated inside the approximately circular area below the nozzle outlets. This result is consistent with the findings of Reichard et al. (1992) in which even at a wind speed of 4 m/s, water droplets with a size of 200 μm and coarser did not drift farther than 0.3 m below the nozzle. At different forward speeds, most spray particles over 200 μm were concentrated inside the spray area with no drift. According to Nowatzki et. al (2017), drift is far less likely to be a problem when droplets are 200 microns or larger, which is why the maximum drift distance is near drift (<5 m) even at 8 km/h traveling speed of the tractor. Moreover, droplets with a diameter of 200 microns travelled less than 0.64 m from the nozzle which is accurate to the computed drift distance at different forward speeds.

Spray Drift Characteristics at Different Wind Angles of Attack

The resultant velocity of the wind (v_R) relative to the tractor moving at 8 km/h at various wind directions shown in Figure 3 is tabulated in TABLE 3. The resultant velocity of the air relative to the tractor decreases from 0° to 180° wind direction with respect to the positive z-axis.

TABLE 3. Resultant velocity of the air with respect to the tractor at different wind directions.

Wind direction WRT Positive z-axis (°)	v_R (m/s)	Angle of v_R WRT positive z-axis (°)
0	3.72	0
45	3.45	17.92
90	2.68	34.05
135	1.57	42.46
180	0.72	0

As the direction of the wind deviates clockwise from the tractor, the resultant velocity of the air decreases. Maximum generated resultant wind velocity was 3.72 m/s at 0° wind angle where the wind blows opposite the direction of the tractor while resultant wind velocity at 180° wind angle is only 0.72 m/s resulting to no occurrence of spray drift. Since the resultant velocity of air with respect to tractor, V_R, decreases as the wind deviates from the positive z-axis, the general trend of drift distances is also decreasing. However, due to the obstruction of the tractor to the wind coming from different angles, the orientation and shape of the wake area also change, resulting in a non-linear decrease of spray drift from each nozzle, as visualized in FIGURE 13. Droplet Z position at different wind directions. at different wind angles.
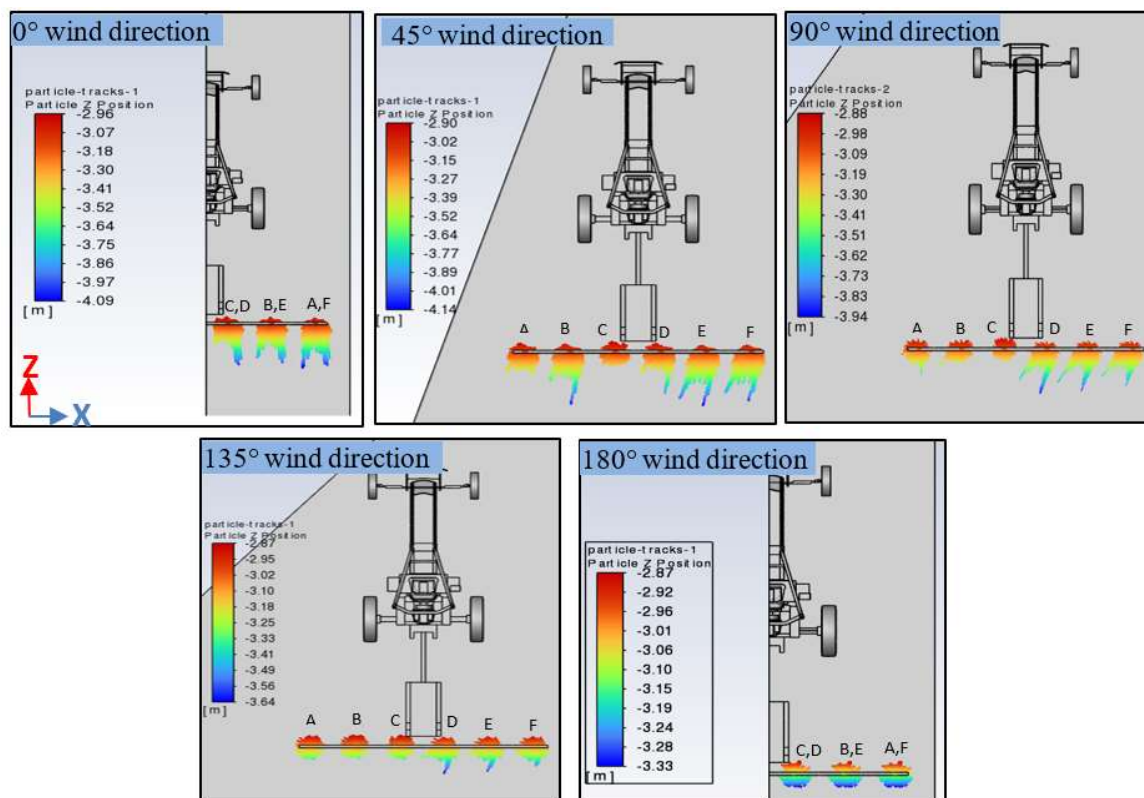

FIGURE 13. Droplet Z position at different wind directions.

It can be observed that the drift distances from each nozzle vary at different wind directions. Spray droplets are drifted along the direction of resultant wind velocity. At 0° wind direction, the drift distances from the nozzles were relatively more uniform with the nozzles at the ends of the boom experiencing slightly farther drift distance. At 45° wind direction, nozzles B, D, E, and F have relatively longer drift distances than nozzles A and C. At 90° wind direction, longer spray drifts are more observable at nozzles D, E, and F. At this angle, the wind speed is higher than 1.5 m/s, and according to the mathematical model assumption used by Renaudo et al. (2023), the turbulent dispersion along the wind direction follows a Gaussian distribution whilst dispersion along the z-axis is assumed negligible as convective effects of the wind transport are greater than the turbulent dispersion effect. On the other hand, short to no drift can be noticed at 135° and at 180° wind direction. Changes in the wake region is visualized in FIGURE 14 at different wind directions to show how the drift distances from each nozzle vary due to the changes in the wake. At 90° wind direction, spray drift is minimal at the nozzles covered by the wake of the tractor components, which block the incoming air, such as the tractor wheels and the boom sprayer tank.
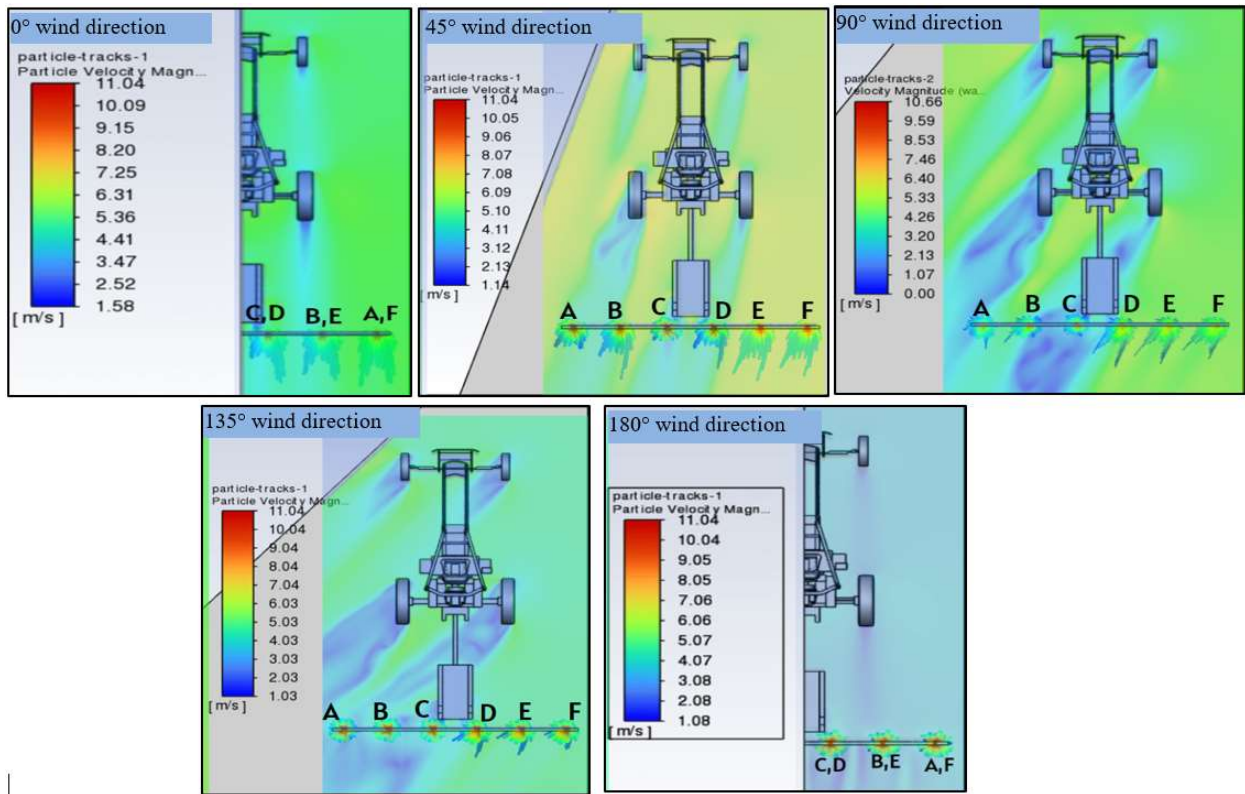
FIGURE 14. Wind velocity profile overlaid on droplet tracks at different wind directions.

The maximum drift distances from each nozzle are shown in TABLE 4. Maximum drift distances at 0° wind direction are more uniform ranging from 0.62 m to 0.76 m while at 180° where V_R is lowest, negligible spray droplets drifted from all the nozzles. Spray drift from end nozzle was consistently decreasing since it was more exposed to the free flow of wind at different wind directions. Noticeably, nozzle C has negligible spray drift at wind angles of 45° to 180° since it is close to the sprayer tank, while nozzles A and B experienced negligible drift at 135° to 180°. Also, drift distances at 45°, 90° and 135° were less uniform among all the nozzles.

TABLE 4. Maximum drift distance from the nozzles at different wind angles.

Angle of attack with resp. to negative z-axis (°)	Maximum drift distance (m)					
	Nozzle A	Nozzle B	Nozzle C	Nozzle D	Nozzle E	Nozzle F
0	0.76	0.62	0.68	0.68	0.62	0.76
45	0.25	0.74	*	0.54	0.79	0.69
90	0.22	0.29	*	0.60	0.70	0.61
135	*	*	*	0.34	0.29	0.13
180	*	*	*	*	*	*

* negligible spray drift.

Additionally, even though the highest resultant velocity of wind is computed at 0° wind direction, the drift distances from nozzles B and E were higher at 45° wind direction since they are more exposed to the unobstructed wind with a computed drift of 0.74 m and 0.79 m respectively.

The recommended driving speeds are shown in TABLE 5, which is expected to lower the resultant velocity of the wind (Vr) at different wind directions when the wind condition is ideal for spraying at around 1.5 m/s. The spray trajectories from all the nozzles were relatively more uniform when the wind direction was along the tractor's direction. Hence, it is recommended to perform boom spraying at 0° and 180° wind direction and adjust the driving speed as necessary to minimize spray drift further.

TABLE 5. Recommended RB tractor driving speed at different wind direction.

Wind direction (°)	Recommended driving speed (km/h)	V_R at 8 km/h driving speed (m/s)	V_R at recommended driving speed (m/s)	Spray drift
0	4	3.72	2.61	minimal
45	4	3.45	2.42	minimal
90	4	2.68	1.87	minimal
135	5	1. 57	1.11	negligible
180	8	0.72	0.72	negligible

The RB tractor can be operated up to 8 km/h for a more time-efficient spraying with negligible spray drift when the wind direction is at 180°. While at 0° wind direction, the RB tractor must be driven to the minimum recommended driving speed of 4 km/h to minimize spray drift.

CONCLUSIONS

Spray drift characteristics of an RB tractor-trailed boom sprayer were assessed using computational fluid dynamics. First, the aerodynamics of the RB tractor was characterized by analyzing the velocity and turbulent kinetic energy profile in relation to its wake region and by determining its drag coefficient. Furthermore, the spray drift characteristics at different forward speeds and at different wind angles of attack were estimated. Results showed that the wake length of the RB tractor extends beyond five times its length and at its various forward speeds with a top speed of 10.4 km/h, the turbulent kinetic energy profile and velocity profile at the wake has small variation implying that the tractor obstruction to the flow of air does not greatly disturb the airflow at the wake. Moreover, there was negligible spray drift at tractor speeds lower than 4 km/h. The drift of spray droplets when the wind angle of attack changes from 0° to 180° theoretically should decrease, but due to the changes in the wake region of the tractor, the spray drift from each nozzle along the boom exhibited non-uniform drift distances. At light breeze wind conditions, low travel speeds (up to 4 km/h) are recommended at 0° to 90° wind direction to minimize the drift, and at higher travel speeds (up to 8 km/h), it is preferred that the tractor should be operated along with the prevailing wind direction.

ACKNOWLEDGEMENTS

REFERENCES

Al Heidary M, Douzals J, Sinfort C (2020) An attempt to reduce spray drift in wind tunnel by substituting nozzles on the boom. Agricultural Engineering International: CIGR Journal 22 (3):76-84.

Al Heidary M, Douzals J, Sinfort C, Vallet A (2014) Influence of spray characteristics on potential spray drift of field crop sprayers: a literature review. Crop Protection 63: 120–130. https://doi.org/10.1016/J.CROPRO.2014.05.006

AMTEC - Agricultural Machinery Testing and Evaluation Center (2021) Agricultural machinery-four-wheel tractor Oggun. UPLB, College, Laguna: AMTEC.

Baetens K, Nuyttens D, Verboven P, De Schampheleire M, Nicolaï B, Ramon H (2007) Predicting drift from field spraying by means of a 3D computational fluid dynamics model. Computers and Electronics in Agriculture 56(2): 161–173. https://doi.org/10.1016/J.COMPAG.2007.01.009

Baurdoux M, Snelder D, De Snoo G (2004) Pesticides in the Cagayan valley (Philippines): usage, drift patterns and the exposure of farmers differing in income and market access. Communications in agricultural and applied biological sciences 69(4): 765–778.

Cai C, Ming T, Fang W, de Richter R, Peng C (2020) The effect of turbulence induced by different kinds of moving vehicles in street canyons. Sustainable Cities and Society 54: 102015. https://doi.org/10.1016/J.SCS.2020.102015

Chethan CR, Singh PK, Dubey RP, Chander S, Ghosh D (2019) Herbicide application methodologies: influence of nozzle selection, droplet size and spray drift on effective spraying–a review. Innovative Farming 4(1): 045-053.

Djouhri M, Loubet B, Bedos C, Dages C, Douzals JP, Voltz M (2023) ADDI-Spraydrift: a comprehensive model of pesticide spray drift with an assessment in vineyards. Biosystems Engineering 231: 57–77. https://doi.org/10.1016/J.BIOSYSTEMSENG.2023.05.008

Eckert JJ, Santiciolli FM, Costa E dos S, Corrêa FC, Dionísio HJ, Dedini FG (2014) Vehicle gear shifting co-simulation to optimize performance and fuel consumption in the Brazilian standard urban driving cycle. Blucher Engineering Proceedings 615–631. https://doi.org/10.5151/ENGPRO-SIMEA2014-81

Hong SW, Park J, Jeong H, Lee S, Choi L, Zhao L, Zhu H (2021) Fluid dynamic approaches for prediction of spray drift from ground pesticide applications: a review. Agronomy 11(6): 1182. https://doi.org/10.3390/AGRONOMY11061182

Jomantas T, Lekavičienė K, Steponavičius D, Andriušis A, Zaleckas E, Zinkevičius R, Popescu CV, Salceanu C, Ignatavičius J, Kemzūraitė A (2023) The influence of newly developed spray drift reduction agents on drift mitigation by means of wind tunnel and field evaluation methods. Agriculture 13(2): 349. http://dx.doi.org/10.3390/agriculture13020349

Kruger G, Klein R, Ogg C, Vieira B (2019) Spray drift of pesticides. Nebraska Extension. Available: https://extensionpublications.unl.edu/assets/html/g1773/build/g1773.htm

Lechler Inc. (n.d.). Precision spray nozzles and accessories catalog. Available: https://www.lechlerusa.com/fileadmin/media-usa/Literature/Catalog/CATALOG_501.pdf. Accessed March 8, 2021.

Lu JL (2017) Assessment of pesticide-related pollution and occupational health of vegetable farmers in Benguet province, Philippines. Journal of Health & Pollution 7(16): 49–57. https://doi.org/10.5696/2156-9614-7.16.49

Musiu EM, Qi L, Wu Y (2019) Spray deposition and distribution on the targets and losses to the ground as affected by application volume rate, airflow rate and target position. Crop Protection 116: 170–180. https://doi.org/10.1016/J.CROPRO.2018.10.019

Nowatzki J, Hofman V, Solseng S (2017) Review on reducing spray drift. North Dakota State University Extension. Available: https://www.ag.ndsu.edu/publications/crops/reducing-spray-drift

Reichard DL, Zhu H, Fox RD, Brazee RD (1992) Computer simulation of variables that influence spray drift. Transactions of the ASAE 35(5): 1401–1407. https://doi.org/10.13031/2013.28747

Renaudo CA, Bertin DE, Bucalá V (2023) A hybrid Lagrangian-dispersion model for spray drift prediction applied to horizontal boom sprayers. Journal of Aerosol Science 173: 106210. https://doi.org/10.1016/J.JAEROSCI.2023.106210

Sarkar S, Thummar K, Shah N, Vagrecha V (2019) A review paper on aerodynamic drag reduction and CFD analysis of vehicles. International Research Journal of Engineering and Technology. Available: www.irjet.net

Sarker S, Akbor MA, Nahar A, Hasan M, Islam ARMT, Siddique MAB (2021) Level of pesticides contamination in the major river systems: a review on South Asian countries perspective. Heliyon 7(6): e07270. https://doi.org/10.1016/J.HELIYON.2021.E07270

Schönenberger UT, Simon J, Stamm C (2022) Are spray drift losses to agricultural roads more important for surface water contamination than direct drift to surface waters? Science of The Total Environment 809: 151102. https://doi.org/10.1016/J.SCITOTENV.2021.151102

Tsay J− R, Liang L − S, Lu L − H (2004) Evaluation of an air−assisted boom spraying system under a no−canopy condition using CFD simulation. Transactions of the ASAE 47(6): 1887–1897. Available: https://sci-hub.do/https://elibrary.asabe.org/abstract.asp?aid=17797

Wieringa J (1992) Updating the Davenport roughness classification. Journal of Wind Engineering and Industrial Aerodynamics 41(1–3): 357–368. https://doi.org/10.1016/0167-6105(92)90434-C

Xue S, Xi X, Lan Z, Wen R, Ma X (2021) Longitudinal drift behaviors and spatial transport efficiency for spraying pesticide droplets. International Journal of Heat and Mass Transfer 177: 121516. https://doi.org/10.1016/J.IJHEATMASSTRANSFER.2021.121516

Zhong W, Zhou H, Jia W, Xue F (2020) Numerical simulation on deposition of atomization droplet of air-assist boom spraying in air flow. Journal of Physics: Conference Series 1637: 012145. https://doi.org/10.1088/1742-6596/1637/1/012145